# Quantum Mechanical Modeling of Condensed Matter Systems

Authors:
**Samuel Skriloff** (Nanoscale Engineering/Applied Mathematics, Soph.)
**Steven Gassner** (Nanoscale Science/Applied Mathematics, Soph.)
**Sean Gibbons** (Nanoscale Engineering/Applied Mathematics, Soph.)

Advisor: Dr. Andrea Dziubek

SUNY Polytechnic Institute
Colleges of Nanoscale Science and Engineering

# Contents

**List of Abbreviations**

DOS ≡ Density of States

LDOS ≡ Local Density of States

TDSE ≡ Time Dependent Schrödinger Equation

TISE ≡ Time Independent Schrödinger Equation

**Nomenclature**

The meaning of symbols and physical constants are mentioned as they are introduced throughout the report.

**List of Figures**

# 1 Project Definition

The aim of this project is to survey numerical techniques for the simulation of quantum mechanical condensed matter systems. Starting from the basics of the Time Independent Schrödinger Equation and discretizing space into a lattice, a matrix equation for the all-important Hamiltonian is derived, and its relevance is studied in a handful of demonstrative systems. An additional goal of this project is to explore techniques for the reduction of exceedingly large Hamiltonian matrices into forms that are much less computationally intensive. This model reduction is achieved through the analysis of physical symmetries as well as through linear algebra methods.

# 2 Physical Problem

## 2.1 Quantum Physics (Simplified)

(Note: In this discussion, we set the reduced Planck's constant $\hbar = 1$.)

Quantum mechanical systems are characterized by *observables*, numerical quantities which can be directly measured from the system. Examples of observables include position ($x$), linear momentum ($p$), and energy ($E$).

At sufficiently small scales, it becomes apparent that such observables can only take certain discrete values. For example, a given particle may sometimes be observed to have an energy of 1 eV or 2 eV, but may never be observed to have any values of energy in between. We then say that properties like the energy of a system are *quantized*, and are limited to a discrete set of possible values when observed.

As an example, let us discuss a simplified version of a famous experiment done by Otto Stern and Walther Gerlach that discovered the property of *spin* in subatomic particles. Although spin is a purely quantum mechanical phenomenon, it can be understood heuristically as the literal "spinning" of a charged particle, such as an electron. Classically, the angular momentum of a spinning charged sphere produces a magnetic field analogous to a bar magnet, with a north and south pole (Figure 1).

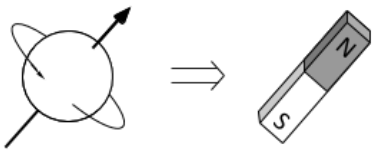


Figure 1: The spin of a charged particle is analogous to a tiny bar magnet

Let us imagine an apparatus such as that in Figure 2, with a strong magnetic field $\boldsymbol{B}$ applied as shown. Let us imagine shooting a tiny bar magnet through this apparatus. One would expect the magnet to be deflected by the magnetic field, and if a detector screen is placed behind the apparatus, the magnet should leave a mark that is higher or lower than the position straight ahead of its original trajectory. (This is under the crucial assumption that the magnetic field $\boldsymbol{B}$ does not rotate the magnet in any way, and that the deflection of the magnet is dependent only on its initial orientation when shot through the detector. Keep in mind that this is in analogy to the *angular momentum* of a tiny particle, which we assume would be negligibly changed during its brief trip through the apparatus.)

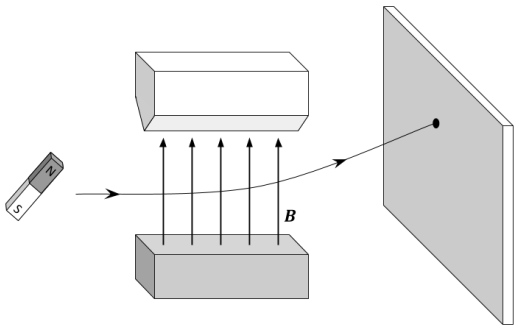


Figure 2: Simplified schematic of the apparatus used in the Stern-Gerlach experiment

Let us now consider a variety of orientations for this bar magnet, orientations (a), (b), and (c) as shown in Figure 3. We would expect varying angles for the bar magnet to result in varying degrees of deflection. Magnets with their north pole pointing in the direction of the magnetic field lines are expected to deflect further upward, while magnets pointing in the opposite direction are expected to deflect further downward. Thus, we can treat this apparatus as a *measuring instrument* for the orientation of a small bar magnet! A simple calculation (which we will not bother with here) could easily connect the detector position of a bar magnet with its angle relative to some axis, and we can thus easily determine from the detector screen approximately what angle the bar magnet makes with the vertical direction.

Now, what happens when we use this apparatus to measure the *spin* of subatomic particles? Let us imagine shooting a beam of electrons through our apparatus. (Stern and Gerlach used silver atoms, but since the angular momentum of silver is highly influenced by its lone valence electron, the principle remains the same if we instead discuss electrons.) The result from a beam of electrons is quite peculiar (Figure 4). Two very distinct bands of markings appear on the detector screen. There seem to be only two possible measured orientations for our electrons! In contrast to the bar magnets, which we presume could be in any random orientation and thus would create a broad, continuous distribution of marks on the detector screen, each of our electrons is only measured to be in one of two very precise orientations with respect to apparatus!

The conclusion to be drawn from the Stern-Gerlach experiment, and

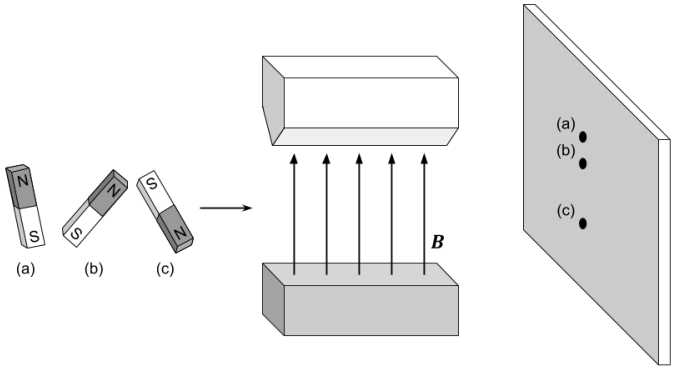


Figure 3: The expected trajectories for three bar magnet orientations (a), (b), and (c), with detector positions labeled accordingly

countless other experiments studying nature at its smallest scales, is that observable values in Nature are *quantized*. In the case of our electron spin, we say that an electron's spin can be observed to be $+1/2$ ("spin up") or $-1/2$ ("spin down"), and *no values of spin in between*. This quantization is one of the fundamental ideas of quantum mechanics.

Another fundamental property of quantum mechanics is that of *probability*. We will extend our simplified example of the Stern-Gerlach experiment to make this notion of probability seem as natural as possible.

Imagine that we take all the "spin up" electrons from our experiment and shoot them through an identical measuring apparatus. We expect all the electrons to be deflected upward, and they do (Figure 5). Now let us imagine that the new detector is aligned *perpendicularly* to the axis along which our original $\boldsymbol{B}$ was pointing. Classically speaking, the component of a magnetic moment along an axis perpendicular to the direction of the magnetic moment is zero. But as we saw in our experiment, zero is not an allowed value! Only values of $+1/2$ or $-1/2$ can be measured! Nature thus has to choose between one of these values for the measured spin. So what is she to do?

What Nature does in this case is something that has led many great physicists to feel very uneasy about quantum mechanics (including Albert Einstein, one of the founding fathers of the field). Nature plays dice. In this idealized scenario, where the detector is perfectly orthogonal to the direction of the incident spins, the only prediction we can make is that half

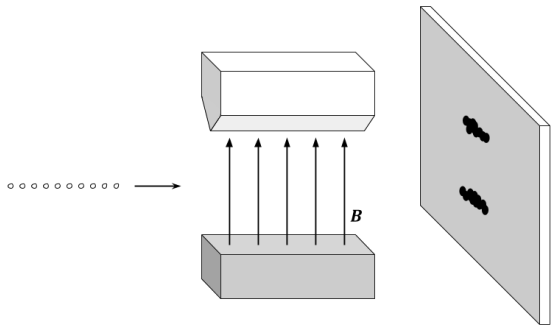


Figure 4: The result when electrons are shot through our apparatus

will be deflected to the left and half will be deflected to the right. According to quantum mechanics, in this scenario, nothing can be done to predict with certainty what the spin of any particular electron will come out to be–only the *probability* of a certain outcome can be known. Therein lies the probabilistic nature of quantum theory. (It is a little more complicated than this, but further details are discussed in the next section.)

## 2.2 Probability in Quantum Mechanics

One more important point to be mentioned about quantum mechanics is that the kinds probabilities that Nature uses are quite different from classical probability theory. The difference lies in the use of complex numbers. To calculate probabilities in quantum mechanics, one adds up complex quantities called "amplitudes" and then takes the square modulus of the result to obtain the probability of a particular outcome. This style of probability allows for the peculiar effect of *interference*, in which adding the amplitudes of two related events can actually *decrease* the probability of an outcome relative to its probability when either of the two events is considered separately.

The notation we use here is Dirac notation (a.k.a. "bra-ket" notation), where vectors in a multi-dimensional complex space called a Hilbert space can be written as "kets" (e.g. $|v\rangle$, representing column vectors) and "bras" (e.g. $\langle v|$, representing a complex-conjugated row vector). That is,

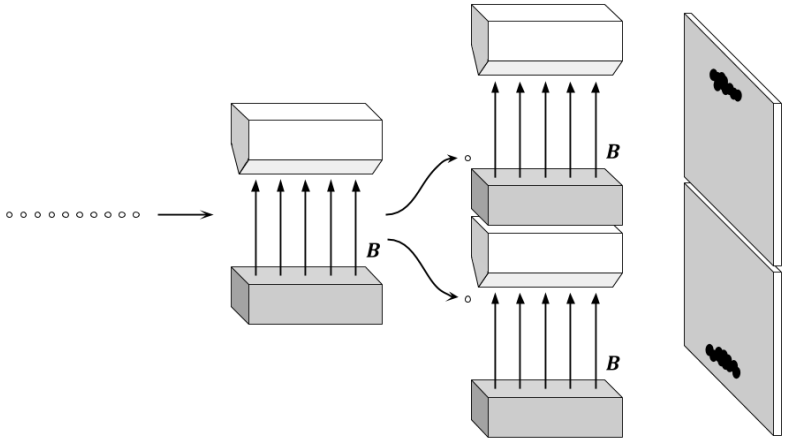


Figure 5: Imagine two more detectors placed in such a way that all "spin up" electrons go to the top one and all "spin down" electrons go through the bottom one

$$|v\rangle := \begin{bmatrix} v_1 \\ \vdots \\ v_n \end{bmatrix} \quad \Rightarrow \quad \langle v| = \begin{bmatrix} v_1^* & \dots & v_n^* \end{bmatrix}. \tag{1}$$

We can thus define the inner product between two vectors as,

$$\langle u|v\rangle = \begin{bmatrix} u_1^* & \dots & u_n^* \end{bmatrix} \begin{bmatrix} v_1 \\ \vdots \\ v_n \end{bmatrix} = u_1^* v_1 + \cdots + u_n^* v_n \tag{2}$$

We represent a quantum state as a vector $|\psi\rangle$ in terms of some basis $\{|a_i\rangle\}$ as follows:

$$|\psi\rangle := \sum_i c_i |a_i\rangle \tag{3}$$

where $c_i \in \mathbb{C}$ is the *probability amplitude* for $|\psi\rangle$ to be observed in state $|a_i\rangle$. The *probability* that $|\psi\rangle$ will be observed in state $|a_i\rangle$ is given by the square modulus $|c_i|^2$. In other words,

$$P_{|\psi\rangle \to |a_i\rangle} := |\langle a_i|\psi\rangle|^2 = |c_i|^2 \tag{4}$$

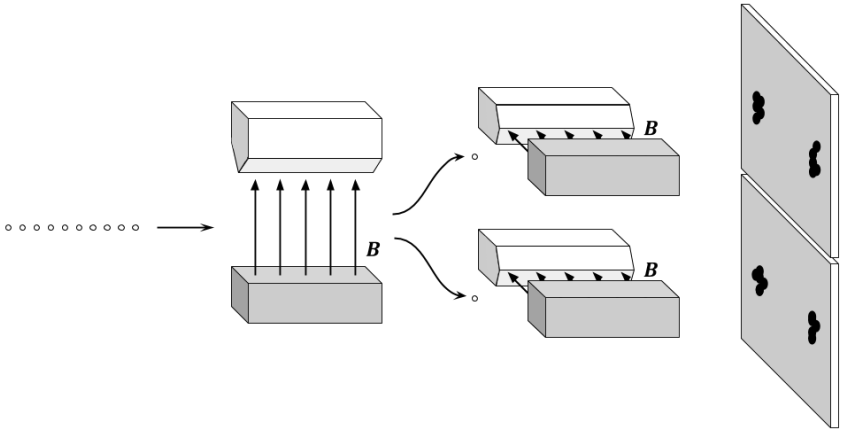


Figure 6: When the two new detectors are made orthogonal to the original detector, an even distribution between "spin left" and "spin right" electrons results

Because the amplitudes $c_i$ are directly related to probabilities, we must require that $|\langle\psi|\psi\rangle|^2 = 1$; in other words, we must require that the sum of the probabilities of the state being found in any of its basis states be equal to unity. Therefore, $6{+}6|\psi\rangle$ is a unit vector.

We will see later on when we discuss applications of the Schrödinger Equation that $\psi$ can be interpreted as a *wavefunction* when expressed in a basis of various position states. This causes the probability of finding the quantum system (for instance, an electron) at a particular position to be defined as the square modulus of a complex-valued wave at that position. Thus, the wavefunction can be used to determine a *probability density function* for the position of a quantum object in a given potential. More on this to come.

# 3 Mathematical Aspects

## 3.1 Operators and Observables

A natural formalism to capture measurements with quantized outcomes is the eigenvalue formalism in matrix mechanics:

$$\hat{O}\psi = O\psi \tag{5}$$

Here, $\hat{O}$ is referred to as the operator with a corresponding observable $O$. The symbol $\psi$ refers generally to the "state" of a quantum system, a mathematical object which contains all the information of a quantum system. Thus, the act of measurement in a quantum system is cast as an eigenvalue problem, where the eigenvalues represent the observables associated with certain eigenstate of that system.

In analogy to the experiment we considered in the previous section, $\hat{O}$ represents the act of sending an electron with initial state $\psi$ through the measuring apparatus, with an observed outcome of $O \in \{-1/2, +1/2\}$.

This becomes a matrix equation when we express the state $\psi$ as a vector in terms of some basis. Let us define,

$$|\uparrow\rangle := \begin{bmatrix} 1 \\ 0 \end{bmatrix}, \qquad |\downarrow\rangle := \begin{bmatrix} 0 \\ 1 \end{bmatrix}. \tag{6}$$

This is a natural choice of a basis, as it consists of two states (spin up and spin down) that are the *eigenstates* of our system. The operator $\hat{O}$ can now be easily written as a diagonal matrix in this basis. We stated earlier that $O$ in Eq. (5) takes on the values $\pm 1/2$. If we assign $+1/2$ as the observable from $|\uparrow\rangle$, and assign $-1/2$ as the observable from $|\downarrow\rangle$, then this implies the following form for $\hat{O}$,

$$\hat{O} := \frac{1}{2}\begin{bmatrix} 1 & 0 \\ 0 & -1 \end{bmatrix}. \tag{7}$$

(In fact, $\hat{O} = \frac{1}{2}\sigma_z$ where $\sigma_z$ is one of the famous Pauli spin matrices, derived specifically for this purpose.)

Thus, in general, the state of an electron $|\psi\rangle$ can be written as a linear combination of a "spin up" state $|\uparrow\rangle$ and a "spin down" state $|\downarrow\rangle$, and by applying the operator $\hat{O}$ to $|\psi\rangle$, one can predict the probability that the electron will have a measured spin of $+1/2$ or $-1/2$.

### 3.2 The Schrödinger Equation

The Time-Dependent Schrödinger Equation (TDSE) is a partial differential equation,

$$i\,\frac{\partial \Psi}{\partial t} = \hat{H}\Psi \tag{8}$$

where $\Psi = \Psi(x,t)$ and $\hat{H}$ is the *Hamiltonian operator*. Borrowed from classical mechanics, the Hamiltonian contains information about the total energy of a system. It can be decomposed into a kinetic energy operator and potential energy operator as follows,

$$\hat{H} = \hat{T} + \hat{V} = -\frac{1}{2m}\frac{\partial^2}{\partial x^2} + V(x) \tag{9}$$

where $V(x)$ is a space-dependent potential energy function for $\Psi$. Thus, the expanded form of the TDSE reads,

$$-\frac{1}{2m}\frac{\partial^2 \Psi}{\partial x^2} + V(x)\Psi = i\frac{\partial \Psi}{\partial t}. \tag{10}$$

Oftentimes, we are more concerned about the space-dependent properties of $\Psi$ than its time-evolution, so we seek a Time-Independent Schrödinger Equation (TISE). We obtain this by separating variables: assuming $\Psi$ is a product of a space-dependent and time-dependent function,

$$\Psi(x,t) = \psi(x)\,\varphi(t) \tag{11}$$

Eq. (8) splits, (letting $\dot{\varphi} := \frac{d\varphi}{dt}$)

$$i\dot{\varphi} = E\varphi\,, \qquad -\frac{1}{2m}\ddot{\psi} + V(x)\psi = E\psi \tag{12}$$

Remembering that the Hamiltonian accounts for the total energy of the system, we use the system's total energy $E$ as the separation constant. The solution to the left-side equation in (11) is the complex exponential $\varphi(t) = \varphi_0 e^{iEt}$, meaning that the time evolution of a state can be thought of as a complex rotation with a frequency dependent on the state's total energy E. The right-side equation in (11) is the TISE we seek, which can be written in terms of $\hat{H}$ as an eigenvalue equation:

$$\hat{H}\psi = E\psi \tag{13}$$

### 3.3 The TISE as an Eigenvalue Problem

Let us rewrite Eq. (13) in terms of "kets" from before,

$$\hat{H}|\psi_n\rangle = E_n|\psi_n\rangle. \tag{14}$$

We use $n$ to index the $n$-th eigenstate $|\psi_n\rangle$ with corresponding eigenvalue $E_n$. The eigenstates of the Hamiltonian represent characteristic states of the system (e.g. "spin up" or "spin down" in our introductory experiment) and the eigenvalues represent the observable quantities corresponding to those states (e.g. $+1/2$ for "spin up" and $-1/2$ for "spin down").

Remembering that we can express a given $|\psi\rangle$ in terms of any basis, like any eigenvalue problem, we can choose a convenient basis formed by the eigenstates (analogous to eigenvectors) of $\hat{H}$,

$$|\psi\rangle := \sum_n c_n|\psi_n\rangle \tag{15}$$

making $\hat{H}$ a diagonal matrix,

$$\left[\hat{H}\right]_{\{|\psi_n\rangle\}} = \begin{bmatrix} E_1 & & \\ & \ddots & \\ & & E_n \end{bmatrix}. \tag{16}$$

Much of the process for numerically solving problems in quantum systems boils down to simplifying $\hat{H}$. See section 9 for more details.

### 3.4 $V(x)$ and the Wavefunction

To illustrate the form of the wavefunction in various potentials, let us rearrange the right-side equation in (12) as follows,

$$\ddot{\psi} = 2m(V(x) - E)\psi \tag{17}$$

This is a second-order linear ODE in $\psi$, with a proportionality constant dependent on the difference between the potential energy and the system's total energy at each point. Let us assign a name to this proportionality constant,

$$k^2 := 2m(V(x) - E) \quad \Rightarrow \quad \ddot{\psi} = k^2\psi \tag{18}$$

and solve the ODE in its most general form,

$$\psi(x) = C_1\, e^{kx} + C_2\, e^{-kx}. \tag{19}$$

Consider the following statements,

$$\begin{aligned} V(x) > E \;\; &\Rightarrow \;\; k^2 > 0 \;\; \Rightarrow \;\; \mathrm{Im}(k) = 0. \\ V(x) < E \;\; &\Rightarrow \;\; k^2 < 0 \;\; \Rightarrow \;\; \mathrm{Re}(k) = 0. \end{aligned} \tag{20}$$

In other words, if the potential in a given region exceeds the total energy of the wavefunction, $k$ is purely real, and thus $\psi$ will take the form of an exponential growth or decay in this region; if the total energy exceeds the potential, then $k$ is purely imaginary, and $\psi$ will take the form of a superposition of sinusoidal waves. Simply put, a wavefunction will oscillate in areas where it has an excess of energy and decay in areas where it does not.

Recall from Section 2 that if $|\psi\rangle$ represents a quantum state in terms of some basis, then it must satisfy $|\langle\psi|\psi\rangle|^2 = 1$. If we choose a basis of infinitesimally small regions in a 1-dimensional space, we can express this normalization condition as an integral,

$$\langle\psi|\psi\rangle = \sum_n \psi_n^* \psi_n = 1 \quad \longrightarrow \quad \int_{-\infty}^{+\infty} \psi^*(x)\psi(x)dx = 1. \tag{21}$$

This integral condition simply states that the probability density function given by the square modulus of the wavefunction must be properly normalized; its integral across its whole domain must converge to 1.

Knowing (20) and (21) is enough to qualitatively predict the form of the wavefunction (or at least the probability function associated with the wavefunction) of a quantum system given its total energy and a potential energy landscape. One simply has to put together sinusoids and exponential curves according to (20) in a way that ensures the absolute area under the curve converges to unity according to (21). Figure 7 illustrates this.

### 3.5 Analytical Solutions of the TISE: Infinite Square Well

Let us move on to a two-dimensional case, applying the principles from the previous section. In two dimensions, the Hamiltonian operator takes the following form,

$$\hat{H} = -\frac{1}{2m}\left(\frac{\partial^2}{\partial x^2} + \frac{\partial^2}{\partial y^2}\right) + V(x, y). \tag{22}$$

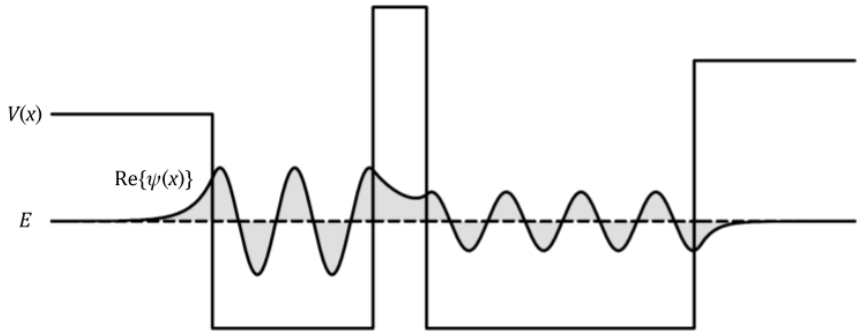


Figure 7: A qualitative visualization of the real component of a wavefunction $\psi(x)$ with energy $E$ in a potential $V(x)$. Note the oscillatory behavior of $\psi(x)$ in regions where $V(x) < E$ and the exponential decays where $V(x) > E$. Note also that the shaded area is finite.

Let us consider a two-dimensional "box," with rigid walls that no particle can escape from. This environment an *infinite square well potential*, where $V$ is 0 inside the box and infinitely large elsewhere. Explicitly,

$$V(x,y) = \begin{cases} 0, & \forall (x,y) \in (0,L_x) \times (0,L_y) \\ \infty, & \text{otherwise} \end{cases}. \tag{23}$$

where $L_x$ and $L_y$ are the lengths of the sides of the box in the $x$ and $y$ directions, respectively.

Focusing on the region inside the box (where $V = 0$), the TISE is simple,

$$-\frac{1}{2m}\left(\frac{\partial^2}{\partial x^2} + \frac{\partial^2}{\partial y^2}\right)\psi = E\psi \tag{24}$$

where $\psi = \psi(x,y)$. Separating variables by imposing a solution $\psi(x,y) = \psi_x(x)\psi_y(y)$, the equation turns into two ODEs, one in terms of $x$ and one in terms of $y$. Consider the ODE in $x$. If we define $k_x^2 := 2mE$, the ODE becomes, (with $\psi'' \equiv \frac{d\psi}{dx}$)

$$\psi_x'' = -2mE\psi_x \quad \longrightarrow \quad \psi_x'' = -k_x^2\psi_x. \tag{25}$$

The general solution to this ODE is thus,

$$\psi_x(x) = C_1 \sin(k_x x) + C_2 \cos(k_x x) \tag{26}$$

with $C_1, C_2 \in \mathbb{C}$.

From the nature of our potential, we know that the wavefunction should be zero at the walls of our box, as well as anywhere outside of it. A particle in this box, regardless of its energy, should have zero probability of being found outside. Thus, our boundary conditions are,

$$\psi_x(0) = \psi_x(L_x) = 0. \tag{27}$$

This eliminates the cosine term in our solution in (26), since that term is nonzero at $x = 0$. What it also does is *quantize* the allowed values for $k_x$! To ensure that (27) is satisfied, the following must be true,

$$\psi_x(L_x) = 0 \;\; \Leftrightarrow \;\; C_1 \sin(kL_x) = 0 \;\; \Leftrightarrow \;\; k_x = \frac{n_x \pi}{L_x}, \;\; n_x \in \mathbb{Z}. \tag{28}$$

We now have a discrete set of eigenstates for our infinite square well Hamiltonian! Repeating the same process for solving $\psi_y(y)$, we arrive at the following general solution,

$$\psi(x,y) = \begin{cases} A \sin\left(\dfrac{n_x \pi}{L_x} x\right) \sin\left(\dfrac{n_y \pi}{L_y} y\right), & \forall (x,y) \in (0, L_x) \times (0, L_y) \\ 0, & \text{otherwise} \end{cases} \tag{29}$$

where $A$ is a normalization constant (the product of the $C_1$ terms from $\psi_x$ and $\psi_y$). This normalization constant is found by imposing the following normalization condition,

$$\int_{-\infty}^{+\infty} \int_{-\infty}^{+\infty} \psi^* \psi \, dy \, dx = 1 \tag{30}$$

which implies,

$$A^2 \int_0^{L_x} \int_0^{L_y} \sin^2\left(\frac{n_x \pi}{L_x} x\right) \sin^2\left(\frac{n_y \pi}{L_y} y\right) dy \, dx = 1 \tag{31}$$

and therefore,

$$A = \frac{2}{L}. \tag{32}$$

We can then conclude that the bound eigenstates of our Hamiltonian associated with a two-dimensional infinite square well, indexed by the two *quantum numbers* $n_x$ and $n_y$ and denoted by $\psi_{n_x,n_y}(x,y)$, are as follows,

$$\psi_{n_x,n_y}(x,y) = \frac{2}{L}\sin\left(\frac{n_x\pi}{L_x}x\right)\sin\left(\frac{n_y\pi}{L_y}y\right) \tag{33}$$

$\forall(x,y) \in (0,L_x)\times(0,L_y)$, and $\psi_{n_x,n_y}(x,y) = 0$ otherwise.

### 3.6 Periodic Boundary Condition

Let us impose a periodic boundary condition as follows,

$$\psi(0) = \psi(L), \;\; L \in \mathbb{R} \tag{34}$$

where $L$ is the distance around a loop, or between two sites that are translationally symmetric ($\psi(x)$ at each site is identical). Let us assume the potential is zero everywhere, i.e. $V(x) = 0$. Then the TISE in one dimension reduces to,

$$\ddot{\psi} = -2mE\,\psi. \tag{35}$$

As usual, let us set $k^2 := -2mE$. Then the ODE in (35) is easily integrated, with a general solution of the form,

$$\psi(x) = C_1 e^{ikx} + C_2 e^{-ikx}, \;\; C_1, C_2 \in \mathbb{C}. \tag{36}$$

Imposing our boundary condition, much like the particle in a box, quantizes $k$ into a discrete set of allowed values,

$$\psi(L) = \psi(0) \;\; \Rightarrow \;\; e^{ikL} = 1 = e^{i2\pi n}, \;\; n \in \mathbb{Z} \tag{37}$$

$$k_n = \frac{2\pi n}{L} \tag{38}$$

# 4 Numerical Methods, Algorithm and Programming, Parameter Analysis, and Discussion of Results

## 4.1 Lattice Hamiltonian via Finite Difference Method

In many practical applications, especially in condensed matter physics, it is useful to discretize space into a set of points with a regular spacing. In one dimension, for example, we can use a set of points $\{x_n\}_{n=1,...,N}$ with a regular spacing $a$ such that $x_n + a = x_{n+1}$. Physically, this can correspond to a lattice where each site is at a distance $a$ from each of its neighbors.

If we discretize space as such, then we can express any continuous function $f(x)$ approximately as a discretized function as follows,

$$f(x), \;\; x \in [x_1, x_N] \;\; \longrightarrow \;\; f(x_n) \equiv f_n, \;\; n = 1, ..., N. \tag{39}$$

Using Dirac notation, we can then express a function as a vector of its values $f_n$ at each $x_n$,

$$|f\rangle := \begin{bmatrix} f_1 \\ \vdots \\ f_N \end{bmatrix}. \tag{40}$$

Formally, we should define a basis for this ket $|f\rangle$. We want to define it in terms of an *orthonormal* basis for the space of discretized functions on our one-dimensional interval. That is, we want a set of functions $\{|U_n\rangle\}$ such that,

$$|f\rangle = f_1 \begin{bmatrix} 1 \\ 0 \\ \vdots \\ 0 \end{bmatrix} + f_2 \begin{bmatrix} 0 \\ 1 \\ \vdots \\ 0 \end{bmatrix} + \cdots + f_N \begin{bmatrix} 0 \\ 0 \\ \vdots \\ 1 \end{bmatrix} \equiv f_1|U_1\rangle + \cdots + f_N|U_N\rangle \tag{41}$$

and thus,

$$\langle U_n|f\rangle = f_n, \qquad \langle U_m|U_n\rangle = \delta_{mn} \tag{42}$$

where $\delta_{mn}$ is the Kronecker delta. Recalling our definition for the inner product in the context of functions from Section 2, our goal is to find a set of functions that satisfy,

$$\langle U_n|f\rangle := \int_{-\infty}^{+\infty} U_m^*(x)f(x)dx = f(x_n) \tag{43}$$

which resembles the definition of the Dirac delta function, given by,

$$\int_{-\infty}^{+\infty} \delta(x-x_n)f(x)dx = f(x_n). \tag{44}$$

Therefore, we can formally define our basis as follows,

$$U_n(x) := \delta(x-x_n) \tag{45}$$

Let us now rewrite the TISE in terms of our discretized quantum state $|\psi\rangle$. For notational simplicity, let us denote $(\psi'')_n \equiv \left.\frac{d^2\psi}{dx^2}\right|_{x_n}$ (not to be confused with $\psi_n''$, the second derivative of the component $\psi_n$ with respect to $x$, which is meaningless for our purposes). Then the TISE reads,

$$-\frac{1}{2m}(\psi'')_n + V_n\psi_n = E\psi_n \tag{46}$$

where $V_n \equiv V(x_n)$. Using the finite difference technique, we can discretize $\psi''$ with a step size $a$. Consider,

$$(\psi'')_n \approx \frac{\psi(x_n-a)-2\psi(x_n)+\psi(x_n+a)}{a^2} \equiv \frac{\psi_{n-1}-2\psi_n+\psi_{n+1}}{a^2}. \tag{47}$$

Substituting (45) into (44) and defining $t_0 := \frac{1}{2ma^2}$, we obtain,

$$-t_0\psi_{n-1} + (2t_0+V_n)\psi_n - t_0\psi_{n+1} = E\psi_n. \tag{48}$$

We now have in (46) a form of the TISE that can be easily translated to tridiagonal matrix equation,

$$\begin{bmatrix} (2t_0+V_1) & -t_0 & & & -t_0 \\ \ddots & \ddots & \ddots & & \\ & -t_0 & (2t_0+V_n) & -t_0 & \\ & & \ddots & \ddots & \ddots \\ -t_0 & & & -t_0 & (2t_0+V_N) \end{bmatrix} \begin{bmatrix} \psi_1 \\ \vdots \\ \psi_n \\ \vdots \\ \psi_N \end{bmatrix} = E \begin{bmatrix} \psi_1 \\ \vdots \\ \psi_n \\ \vdots \\ \psi_N \end{bmatrix} \tag{49}$$

that is,

$$\hat{H}|\psi\rangle = E|\psi\rangle \tag{50}$$

where our Hamiltonian operator $\hat{H}$ is recast as a tridiagonal matrix.

This form of the Hamiltonian, resulting from a nearest-neighbor approximation for the second spatial derivative of $\psi$, reduces the TISE to an eigenvalue problem that is easily solved by numerical procedures.

In physical terms, the diagonal elements $2t_0 + V_n$ correspond to the *on-site energy* for the quantum state at a given lattice site, while the off-diagonal elements $-t_0$ correspond to the *hopping energy* required for a state to "hop" between neighboring lattice sites. The elements in the bottom-leftmost and the top-rightmost entries of $\hat{H}$ were added under the assumption of a periodic boundary condition, that is,

$$\text{“}\psi_{N+1}\text{”} = \psi_1. \tag{51}$$

In the absence of a periodic boundary condition, these elements should be removed.

## 4.2 Nested Dissection Method for Scattering and Transmission Models

Consider a device that can be segmented into a finite scattering region (shown in gray) and an arbitrary number of attached leads each consisting of an infinite connected string of identical supercells (the first shown in red) translated by a consistent lateral translation. Each dot represents an atomic tight binding orbital.

When a five-atom high column is used for discretization, the resulting Hamiltonian is a symmetric block tridiagonal matrix as shown in Figure 9, where each diagonal block represents the Hamiltonian of a layer in Figure 8. The i-th diagonal block of the Hamiltonian represents the coupling between atoms in a column. The off-diagonal blocks to its left and right represent coupling from column i to i-1 and i+1 respectively. Both the diagonal and off-diagonal blocks of the Hamiltonian are sparse for most systems which can be approximated as tight binding.

Under the Landauer-Buttiker formalism the infinite lead Hamiltonian does not need to be calculated but can instead be modeled by converting the finite sparse contact cell Hamiltonian into a dense Hamiltonian of the same dimension. This can be understood as the contribution of a "self energy" term ($\Sigma$) corresponding to the resonant energies in the lead allowed under

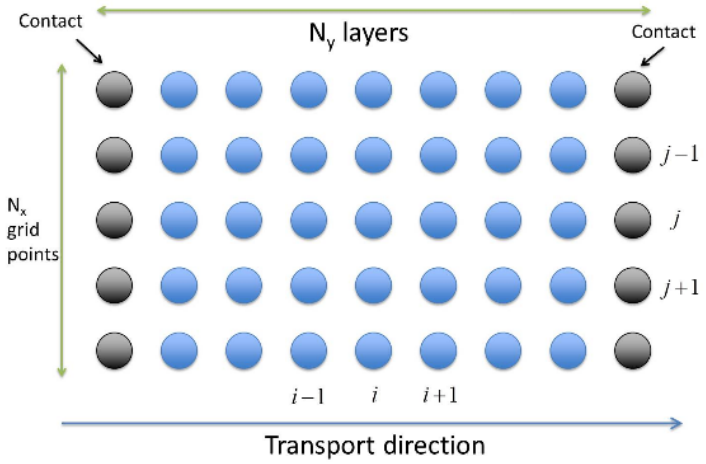


Figure 8: Each dot represents an atomic tight binding orbital.

required commutation with its translation operator. This new Hamiltonian is as such:

$$\hat{H} = H + \sum_i \Sigma^i, \quad \Sigma^i = (V_{ls}^\dagger)_i (G^<)_i (V_{ls})_i \tag{52}$$

where $V_{ls}$ is the matrix of hoppings between the lead and the scattering region. [https://sundoc.bibliothek.uni-halle.de/diss-online/07/07H039/t5.pdf] However this lesser Green matrix ($G^<$) seems to be in inversion of an infinite matrix which is impossible numerically so another method is required for finding it. Typically the method used is the Recursive Green's Function (RGF) however we will instead be using Nested Dissection instead both for efficiency (which will be demonstrated later) as well as its natural interpretation as segmenting of an undirected graph which happens to be the digital model of our lattice.

Note: if the lead structure has a more complex periodic supercell it can be split into isolated sections with the green matrices combining under Dyson's Equation which will not be addressed here.

Nested disection [S. Li, S. Ahmed, G. Klimeck, and E. Darve.Computing entries of the inverse of a sparsematrix using the FIND algorithm.J. Comp. Physics, 227:94089427, 2008] relies on partitioning the device into two completely disjoint regions (L and R) separated by a separator S. (By default a separator is constructed of the same supercell which defines the leads,

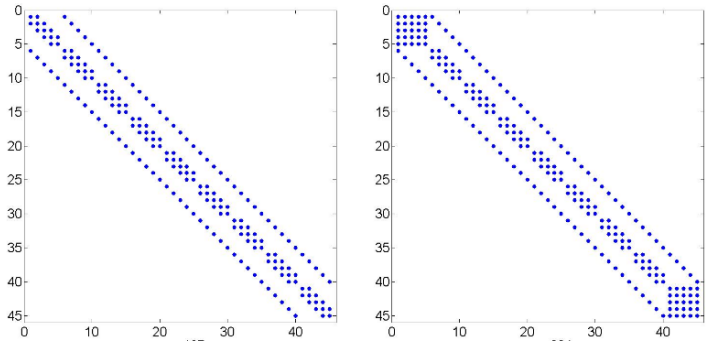

Figure 9: When a five-atom high column is used for discretization, the resulting Hamiltonian is a symmetric block tridiagonal matrix, where each diagonal block represents the Hamiltonian of a layer in Figure 8.

centered in the scattering region.) With this discretization the scattering region Hamiltonian can be written in the block matrix form:

$$A = \begin{bmatrix} A_{LL} & 0 & A_{LS} \\ 0 & A_{RR} & A_{RS} \\ A_{LS}^{\dagger} & A_{RS}^{\dagger} & A_{SS} \end{bmatrix} \tag{53}$$

Note that the matrix remains Hermite. The $LDL^T$ factorization of A is:

$$A = \begin{bmatrix} I & 0 & 0 \\ 0 & I & 0 \\ A_{LS}^{\dagger}A_{LL}^{-1} & A_{RS}^{\dagger}A_{RR}^{-1} & I \end{bmatrix} \begin{bmatrix} A_{LL} & 0 & 0 \\ 0 & A_{RR} & 0 \\ 0 & 0 & \hat{A}_{SS} \end{bmatrix} \begin{bmatrix} I & 0 & A_{LL}^{-1}A_{LS} \\ 0 & I & A_{RR}^{-1}A_{RS} \\ 0 & 0 & I \end{bmatrix} \tag{54}$$

where $\hat{A}_{SS}$ is called the Schurr component:

$$\hat{A}_{SS} = A_{SS} - A_{LS}^{\dagger}A_{LL}^{-1}A_{LS} - A_{RS}^{\dagger}A_{RR}^{-1}A_{RS} \tag{55}$$

The retarded green matrix satisfies the relation [Takahashi et al.]:

$$G^r = (I - L^T)G^r + D^{-1}L^{-1} \tag{56}$$

discretizing $G^r$ on the right side yields:

$$
\begin{aligned}
G^r = &-\begin{bmatrix} A_{LL}^{-1}A_{LS}G_{SL}^r & A_{LL}^{-1}A_{LS}G_{SR}^r & A_{LL}^{-1}A_{LS}G_{SS}^r \\ A_{RR}^{-1}A_{RS}G_{SL}^r & A_{RR}^{-1}A_{RS}G_{SR}^r & A_{RR}^{-1}A_{RS}G_{SS}^r \\ 0 & 0 & 0 \end{bmatrix} \\
&+\begin{bmatrix} A_{LL}^{-1} & 0 & 0 \\ 0 & A_{RR}^{-1} & 0 \\ 0 & 0 & \hat{A}_{SS}^{-1} \end{bmatrix}\begin{bmatrix} I & 0 & 0 \\ 0 & I & 0 \\ -A_{LS}^{\dagger}A_{LL}^{-1} & -A_{RS}^{\dagger}A_{RR}^{-1} & I \end{bmatrix}
\end{aligned} \tag{57}
$$

Therefore the components of $G^r$ can be calculated sequentially:

$$
\begin{aligned}
G_{SS}^r &= \hat{A}_{SS}^{-1}, \\
G_{LS}^r &= -A_{LL}^{-1}A_{LS}G_{SS}^r, \\
G_{RS}^r &= -A_{RR}^{-1}A_{RS}G_{SS}^r, \\
G_{LL}^r &= A_{LL}^{-1} + A_{LL}^{-1}A_{LS}G_{SS}^r A_{LS}^T A_{LL}^{-1}, \\
G_{RR}^r &= A_{RR}^{-1} + A_{RR}^{-1}A_{RS}G_{SS}^r A_{RS}^T A_{RR}^{-1}.
\end{aligned} \tag{58}
$$

The lesser green matrix satisfies the generalized Takahashi relation [Petersen et al.]:

$$
G^< = (I - L^T)G^< + D^{-1}L^{-1}\Sigma^<(G^r)^\dagger \tag{59}
$$

The factorization yields:

$$
\begin{aligned}
G^< = &-\begin{bmatrix} A_{LL}^{-1}A_{LS}G_{SL}^< & A_{LL}^{-1}A_{LS}G_{SR}^< & A_{LL}^{-1}A_{LS}G_{SS}^< \\ A_{RR}^{-1}A_{RS}G_{SL}^< & A_{RR}^{-1}A_{RS}G_{SR}^< & A_{RR}^{-1}A_{RS}G_{SS}^< \\ 0 & 0 & 0 \end{bmatrix} \\
&+\begin{bmatrix} A_{LL}^{-1} & 0 & 0 \\ 0 & A_{RR}^{-1} & 0 \\ 0 & 0 & \hat{A}_{SS}^{-1} \end{bmatrix}\begin{bmatrix} I & 0 & 0 \\ 0 & I & 0 \\ -A_{LS}^{\dagger}A_{LL}^{-1} & -A_{RS}^{\dagger}A_{RR}^{-1} & I \end{bmatrix}\Sigma^<(G^r)^\dagger
\end{aligned} \tag{60}
$$

The components of $G^<$ are as such:

$$
\begin{aligned}
G_{SS}^< &= G_{SS}^r(\Sigma_{SS}^<(G_{SS}^r)^\dagger - A_{LS}^T A_{LL}^{-1}\Sigma_{LL}^<(G_{SL}^r)^\dagger - A_{RS}^T A_{RR}^{-1}\Sigma_{RR}^<(G_{SR}^r)^\dagger), \\
G_{LS}^< &= -A_{LL}^{-1}A_{LS}G_{SS}^< + A_{LL}^{-1}\Sigma_{LL}^<(G_{SL}^r)^\dagger, \\
G_{RS}^< &= -A_{RR}^{-1}A_{RS}G_{SS}^< + A_{RR}^{-1}\Sigma_{RR}^<(G_{SR}^r)^\dagger, \\
G_{LL}^< &= A_{LL}^{-1}\Sigma_{LL}^<(G_{SL}^r)^\dagger + A_{LL}^{-1}A_{LS}G_{LS}^r, \\
G_{RR}^< &= A_{RR}^{-1}\Sigma_{RR}^<(G_{SR}^r)^\dagger + A_{RR}^{-1}A_{RS}G_{RS}^r,
\end{aligned} \tag{61}
$$

Both L and R can be further split in independent processes which reduce $A_{LL}, A_{RR}, G_{RR}$ and $G_{LL}$ even more. Our program continues splitting until regions are only one unit cell thick in either x or y at which point the corresponding A block can be replaced with an easily precalculated default. For this reason other potentially more efficient methods of splitting such as diagonally under the MATIS system [] were not experimented with.

### 4.3 Multi-step Nested Dissection Algorithm and Results

Keeping track of the splitting relies on multilevel binary tree. Thankfully cython allows for easy implementation of undirected graphs as the remarkably efficient c hash tables which allowed us to forego a separate tree building methods in favor of using a grouped version of the device graph itself. However for demonstration purposes we will rely on a more conventional tree as well as the separate clustered graph:

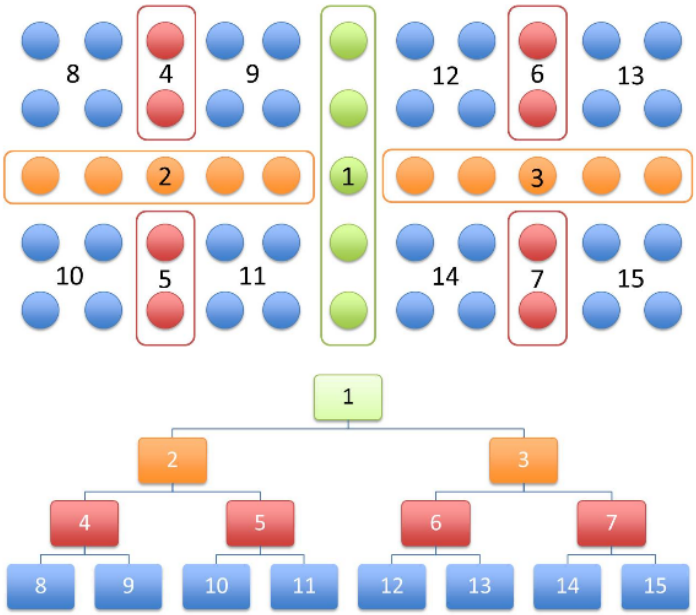


Figure 10: Multi-level binary tree with clustered graph

Based on the hierarchical structure of the tree let $P_i$ denote the set of all clusters that are ancestors of cluster i. For example in the figure $P_6$ = {1,3} and $P_{12}$ = {1,3,6}. Let $A^{(l)}$ denote the matrix A after l levels of

discretization. $A^0$ is therefor A. The first step of the computation is to incorporate all lower level clusters up to level l:

For l in range(1,L-1):

$A^{(l)} = A^{(l-1)}$

for i in clusters in l:

for j in $P_i$:

$\psi_{i,j} = -(A^{(l)}_{i,i})^{-1} A^{(l)}_{i,j}$

for k in $P_i$:

$A^{(l)}_{j,k}$ += $\psi^{\dagger}_{i,j} A^{(l)}_{i,k}$

$A^{(l)}_{k,j} = (A^{(l)}_{j,k})^{\dagger}$

$A^{(l)}_{i,j} = 0$

$A^{(l)}_{j,i} = 0$

Next is the inversion of $A^{(L-1)}$ Since A is block diagonal, this has already been done in the previous step for all blocks other than the first separator. After that $G^{(l)} = (A^{(L-1)})^{-1}$.
Finally diagonal blocks of $G^r$ are extracted:

For l in range(L-2,0,-1):

$G^{(l)} = G^{(l+1)}$

for i in clusters in l:

for j in cluster indicies in $P_i$:

[$G^{(l)}_{i,j}$+=$\psi_{i,k} G^{(l)}_{k,j}$ for k in $P_i$]

$G^{(l)}_{j,i} = (G^{(l)}_{i,j})^{\dagger}$

[$G^{(l)}_{i,i}$+=$\psi_{i,k} G^{(l)}_{k,i}$ for k in $P_i$]

The complexity of this Nested Dissection (specifically with an extended HSC slicing scheme) is here compared to the the more conventional RGF. For this test both methods were used to divide a square lattice of N by N gridpoints. For the purposes of counting steps rather than computing transmission, self energies were ignored. Multiplication of a matrix of dimension a x b matrix with a matrix of dimension b x c was counted as a*b*c total steps and inversion of square matrix of dimension a was counted as $a^3$. Plotted on a logarithmic scale RGF has complexity $O(N^4)$ while Nested Dissection has only $O(N^3)$

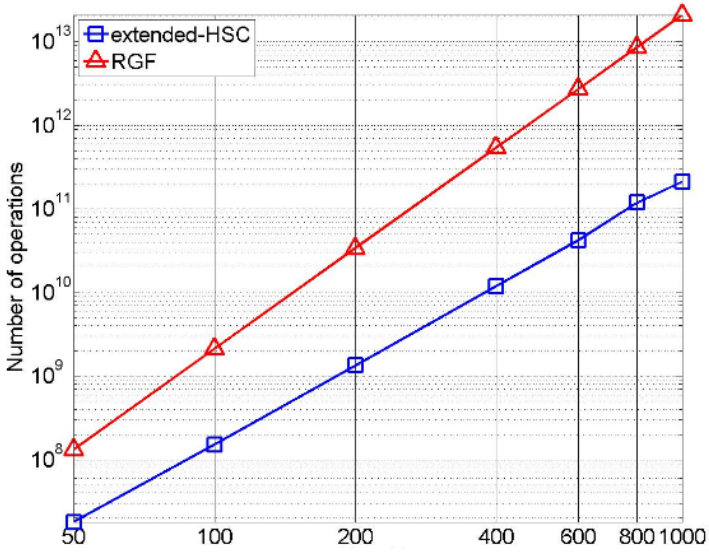


Figure 11: Complexity of extended HSC Nested Dissection versus RGF

# 5 Summary of the Project

The project aimed to give a comprehensive overview of numerical methods of analyzing quantum systems in various lattice geometries and physical scattering regions. Starting from the fundamentals of the Time Independent Schrödinger Equation and obtaining a matrix form for the Hamiltonian, a platform for numerically simulating a wide variety of nanoscale systems was achieved. The project then explored different methods of simplifying the matrix Hamiltonian, using physical symmetries and linear algebra techniques to reduce the model to a less computationally intensive form.

The goal was quite ambitious to try to complete in a month, but plenty of progress was made. A point of improvement, if more time were given for this project, would be to create a more self-contained report with all the preliminary physics necessary for the general mathematically-interested reader to understand the project. Unfortunately, given the depth of this project, this was very difficult to accomplish, but an honest attempt was made to explain the fundamental physics and build up to the main idea behind the project.

# 6 Appendix: Course Evaluation

The authors agree that MAT 460 was an engaging and challenging course worthy of plenty of time commitment, especially during the project phase. Many techniques in numerical mathematics and programming were taught, and the opportunity to apply this to a customized project in a field of science they deeply enjoy is a truly rewarding experience.

Many points of improvement for the course are largely circumstantial. Distance-learning posed a number of difficulties for communication, which is a critical part of any class and any project. However, the professor's willingness to visit Albany on plenty of occasions is deeply appreciated, and it is what gave the class its most indispensable moments for the authors.

The authors agree that perhaps too much time was spent teaching linear algebra and not enough time was spent during the project phase.

Overall, MAT 460 was a rewarding educational experience of which the authors are honored and grateful to have been part.